

## Supporting Information

# Mechanism of CO<sub>2</sub> Photoreduced by Selenium-doped Carbon Nitride with Cobalt Cluster as Cocatalyst

Yuanyuan Hu,<sup>a</sup> Ting Wu,<sup>a</sup> Yi Li,<sup>ab</sup> Yongfan Zhang,<sup>\*ab</sup> Wei Lin<sup>\*ab</sup>

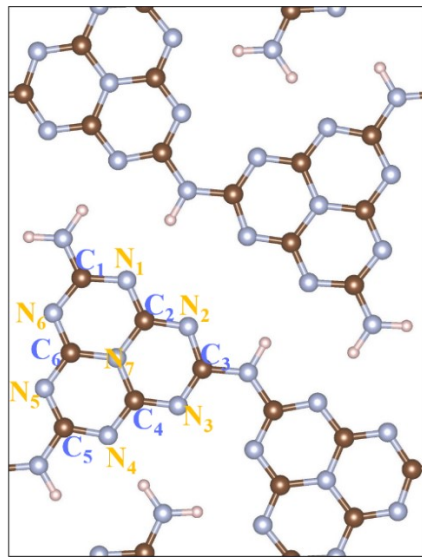
<sup>a</sup> State Key Laboratory of Photocatalysis on Energy and Environment, College of Chemistry, Fuzhou University, Fuzhou 350108, P.R. China

<sup>b</sup> Fujian Provincial Key Laboratory of Theoretical and Computational Chemistry, Xiamen University, Xiamen, Fujian 361005, China

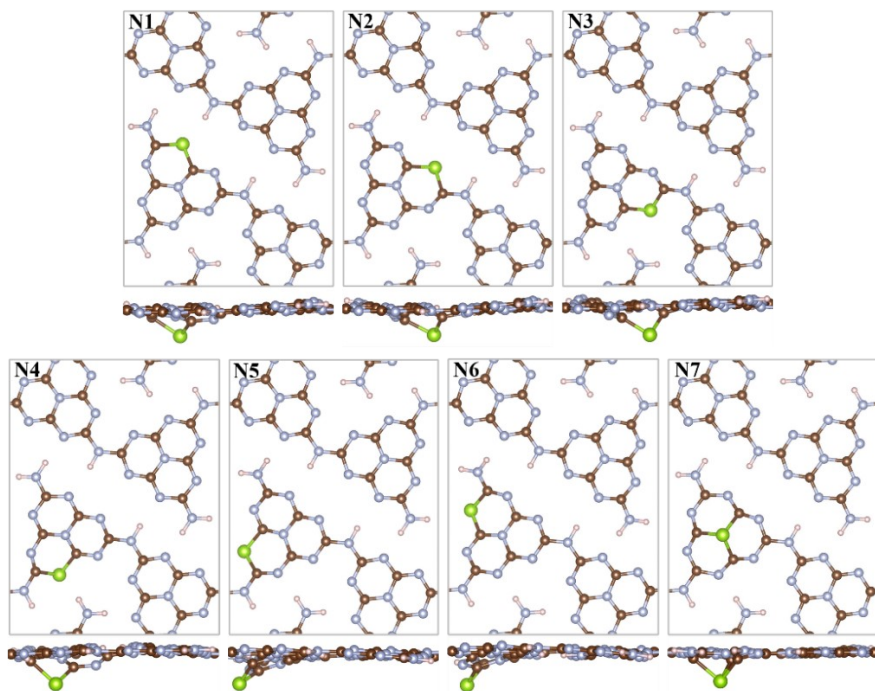
E-mail: zhangyf@fzu.edu.cn (Y. Zhang); wlin@fzu.edu.cn (W. Lin)

**Table S1.** The formation energy ( $E_{form}$ ) of different N and C sites doping systems.

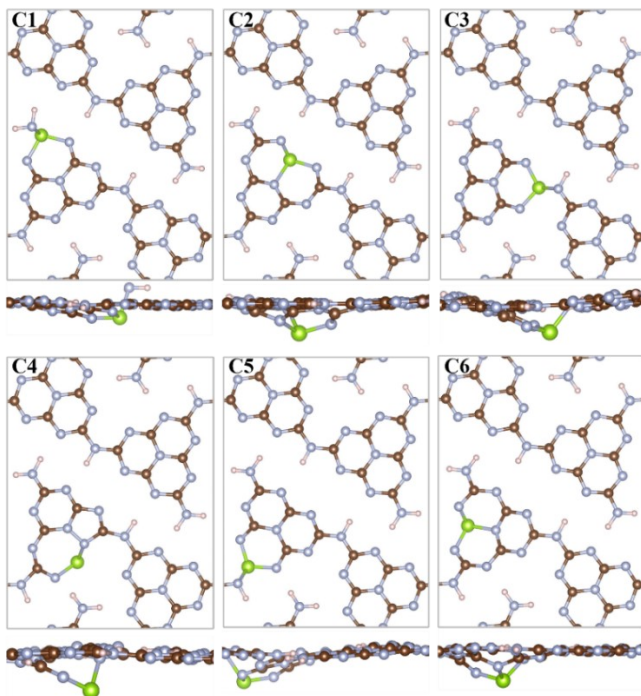
Site	$E_{form}$ (eV)	Site	$E_{form}$ (eV)
N1	-0.37	C1	3.64
N2	-0.54	C2	4.00
N3	-0.44	C3	3.43
N4	-0.25	C4	3.95
N5	-0.50	C5	3.56
N6	-0.33	C6	4.08
N7	0.25		



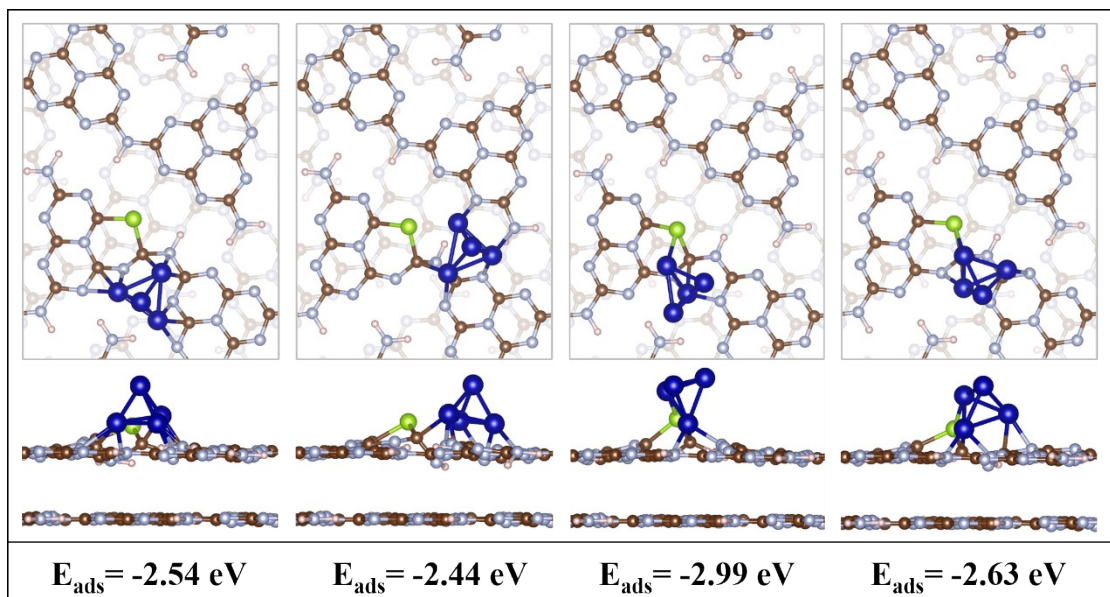
**Fig. S1.** The structural schematic diagrams of Se-decorated melon-based CN. The brown, grey, and light pink balls represent C, N, and H atoms, respectively.



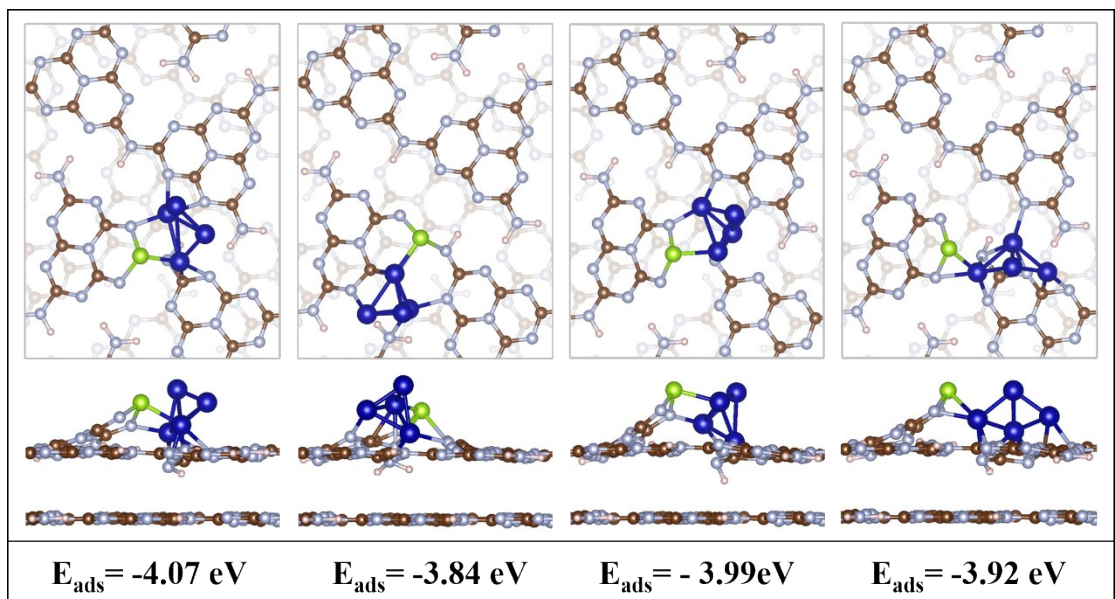
**Fig. S2.** Top and side views of geometric structure of Se-doped CN of the possible doping sites (N1, N2, N3, N4, N5, N6, N7). The brown, grey, light pink and green balls represent C, N, H and Se atoms, respectively.



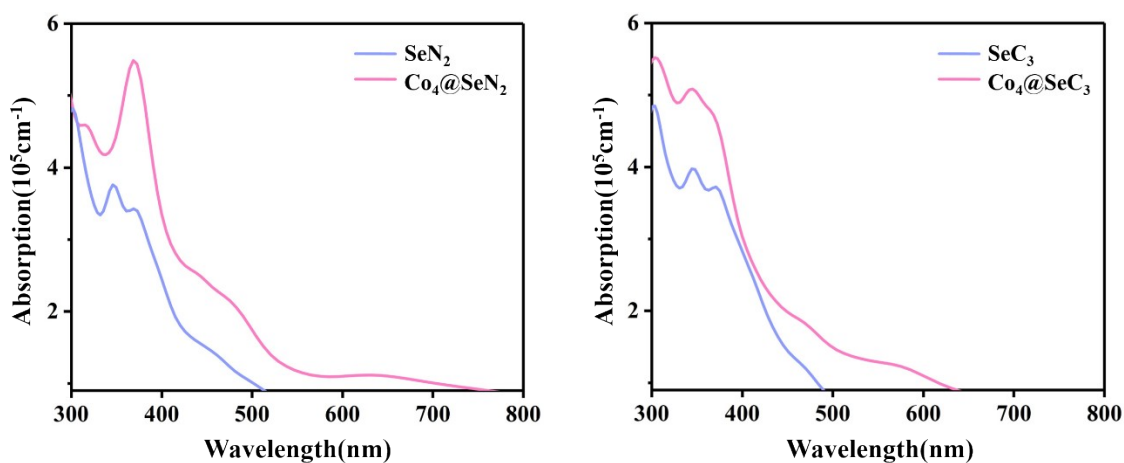
**Fig. S3.** Top and side views of geometric structure of Se-doped CN of the possible doping sites (C1, C2, C3, C4, C5, C6). The brown, grey, light pink and green balls represent C, N, H and Se atoms, respectively.



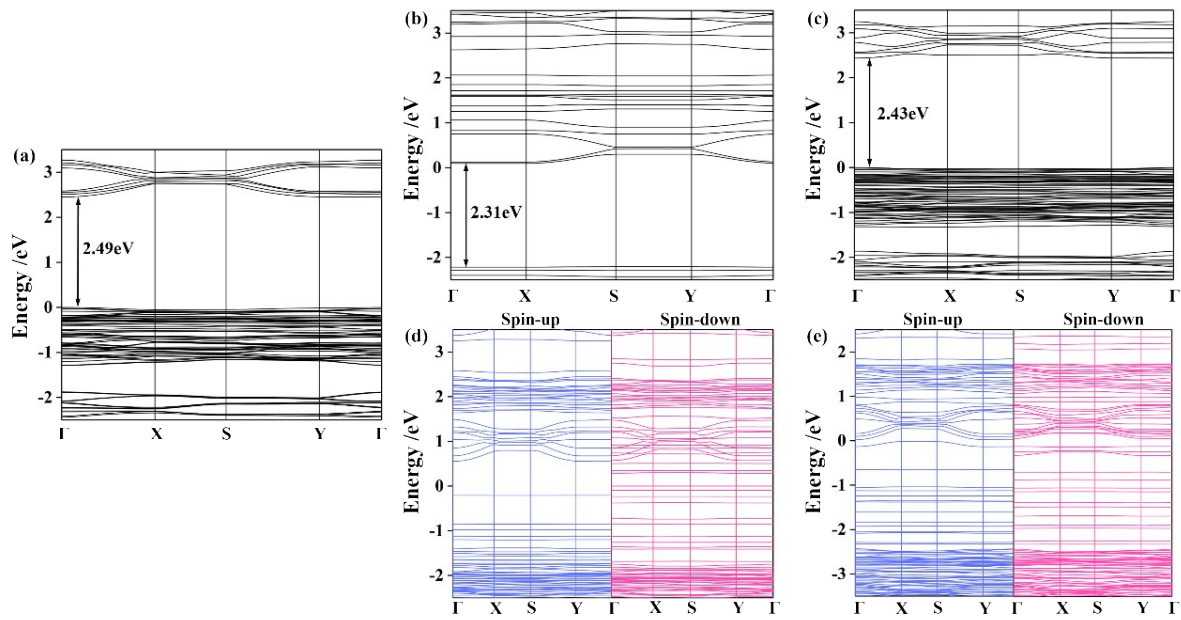
**Fig. S4.** Top and side views of geometric structure of Co<sub>4</sub>@SeN<sub>2</sub>. The brown, grey, light pink, green and blue balls represent C, N, H, Se and Co atoms, respectively.



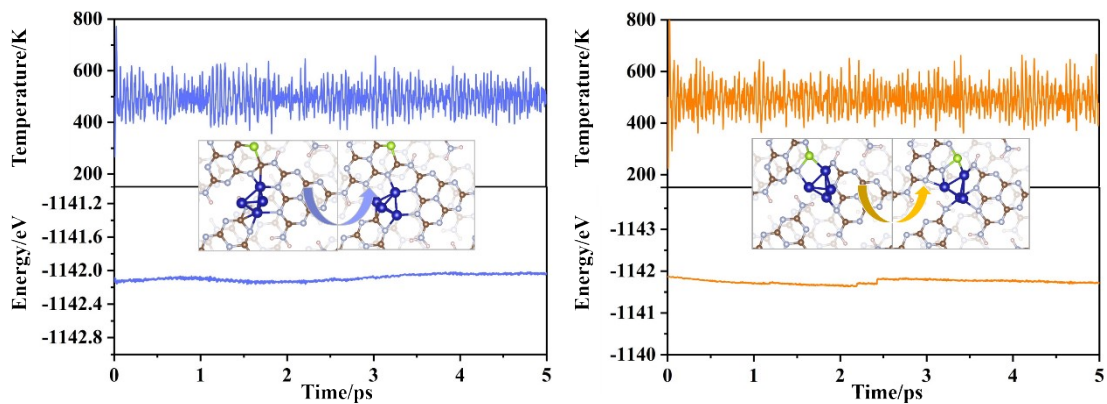
**Fig. S5.** Top and side views of geometric structure of  $\text{Co}_4@\text{SeC}_3$ . The brown, grey, light pink, green and blue balls represent C, N, H, Se and Co atoms, respectively.



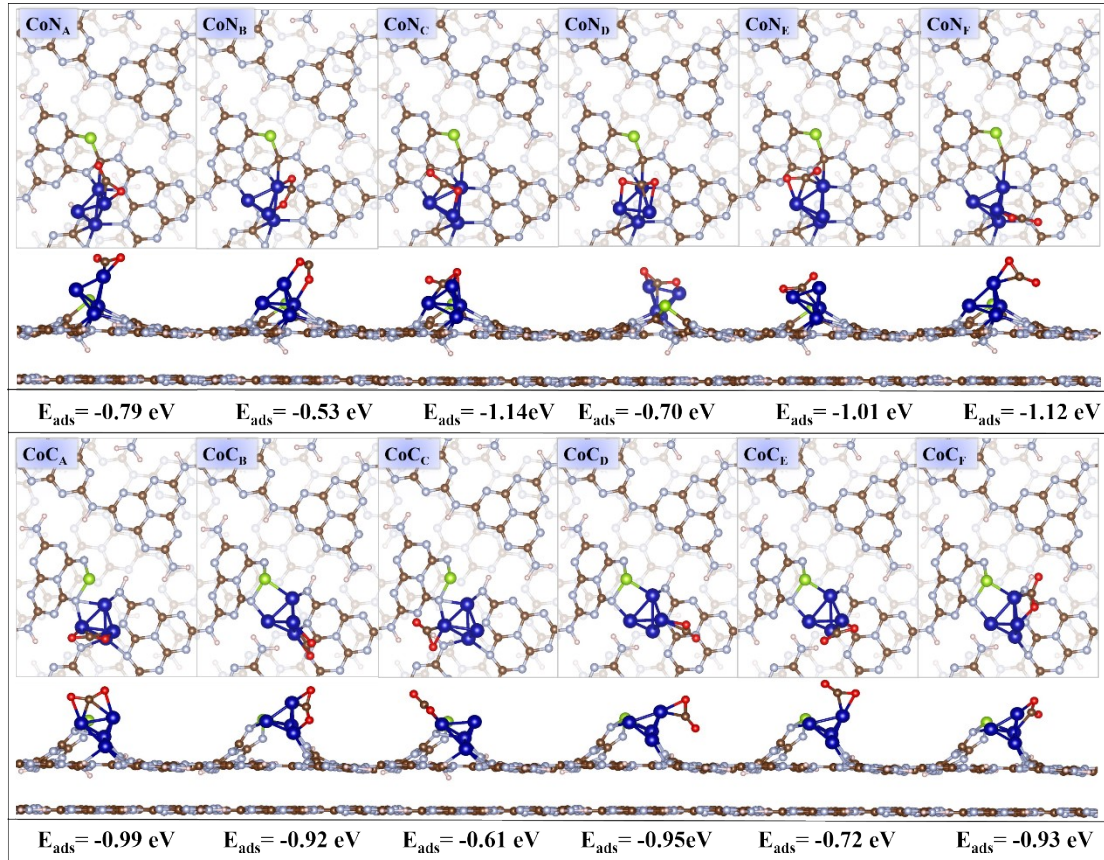
**Fig. S6.** Optical absorption behaviors of photocatalyst.



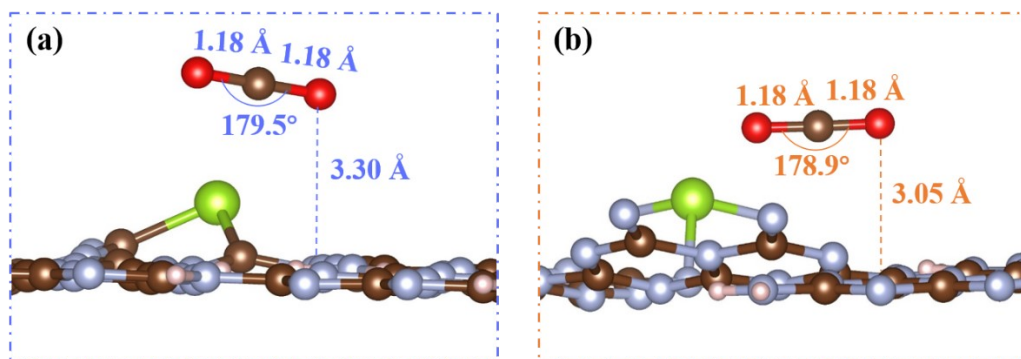
**Fig. S7.** Band structure of (a) pure melon (b)  $\text{SeN}_2$  (c)  $\text{SeC}_3$  (d)  $\text{Co}_4@\text{SeN}_2$  and (e)  $\text{Co}_4@\text{SeC}_3$ .



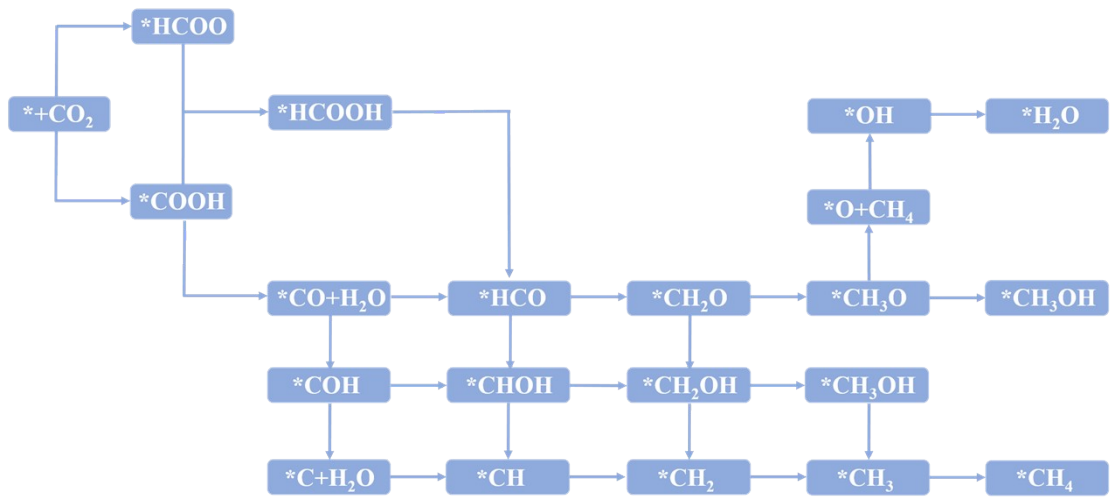
**Fig. S8.** Variations of temperature and energy as a function of (a)  $\text{Co}_4@\text{SeN}_2$  (b)  $\text{Co}_4@\text{SeC}_3$  the time for AIMD simulations of insert is top view of the snapshot of atomic configuration.



**Fig. S9.** The adsorption configuration of  $\text{CO}_2$ , where  $\text{CoN}_\text{A}$ - $\text{CoN}_\text{F}$  are the adsorption situations on  $\text{Co}_4@\text{SeN}_2$ , and  $\text{CoC}_\text{A}$ - $\text{CoC}_\text{F}$  are the adsorption results on  $\text{Co}_4@\text{SeC}_3$ .



**Fig. S10.** The most stable adsorption configurations of  $\text{CO}_2$  in (a)  $\text{SeN}_2$  (b)  $\text{SeC}_3$ . The bluish violet frame indicates n-site doping, and the orange frame indicates C-site doping.



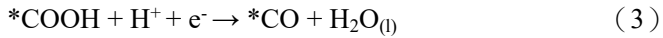
**Fig. S11.** All considered reaction pathways for  $\text{CO}_2$  reduction.

Table S2. Calculated Gibbs free energies,  $T^*S$ , EZPE (in eV) of intermediates in complicated paths

$\text{Co}_4@\text{SeN}_2$	Gibbs energies	$T^*S$ (eV)	$E_{ZPE}$ (eV)	$\text{Co}_4@\text{SeC}_3$	Gibbs energies	$T^*S$ (eV)	$E_{ZPE}$ (eV)
$^*\text{CO}_2$	0.26	0.11	0.31	$^*\text{CO}_2$	0.39	0.18	0.30
$^*\text{COOH}$	0.53	0.15	0.60	$^*\text{COOH}$	0.57	0.13	0.62
$^*\text{HCOO}$	0.45	0.16	0.64	$^*\text{HCOO}$	0.65	0.18	0.73
$^*\text{HCOOH}$	0.84	0.16	0.91	$^*\text{HCOOH}$	0.93	0.48	1.15
$^*\text{CO}$	0.17	0.08	0.20	$^*\text{CO}$	0.16	0.10	0.21
$^*\text{COH}$	0.45	0.11	0.49	$^*\text{COH}$	0.42	0.14	0.49
$^*\text{CHO}$	0.41	0.09	0.44	$^*\text{CHO}$	0.37	0.13	0.43
$^*\text{C}$	0.10	0.02	0.11	$^*\text{C}$	0.22	0.04	0.23
$^*\text{CHOH}$	0.71	0.14	0.77	$^*\text{CHOH}$	0.74	0.13	0.78
$^*\text{CH}_2\text{O}$	0.71	0.15	0.78	$^*\text{CH}_2\text{O}$	0.72	0.13	0.79
$^*\text{CH}_2\text{OH}$	1.01	0.15	1.08	$^*\text{CH}_2\text{OH}$	1.01	0.16	1.09
$^*\text{CH}_3\text{OH}$	1.33	0.21	1.43	$^*\text{CH}_3\text{OH}$	1.04	0.27	1.18
$^*\text{CH}_3\text{O}$	0.96	0.18	1.06	$^*\text{CH}_3\text{O}$	1.03	0.16	1.11
$^*\text{CH}$	0.34	0.14	0.40	$^*\text{CH}$	0.37	0.03	0.38
$^*\text{CH}_2$	0.59	0.05	0.60	$^*\text{CH}_2$	0.62	0.07	0.64
$^*\text{CH}_3$	0.81	0.17	0.90	$^*\text{CH}_3$	0.87	0.12	0.92
$^*\text{CH}_4$	1.07	0.34	1.24	$^*\text{CH}_4$	1.37	0.13	1.43
$^*\text{O}^*$	0.06	0.04	0.07	$^*\text{O}^*$	0.06	0.04	0.08
$^*\text{OH}$	0.30	0.10	0.34	$^*\text{OH}$	0.34	0.07	0.37
$^*\text{H}_2\text{O}$	0.62	0.18	0.70	$^*\text{H}_2\text{O}$	0.57	0.15	0.64

Each step of photochemistry is treated as the simultaneous transfer of proton-electron pairs. For

example, the reaction mechanism for  $\text{CO}_2$  reduction to CO is illustrated below,



where \* stands for the adsorption site. Using the state of gaseous  $\text{CO}_2$  which is unbound above surface as a reference, the Gibbs free energy is represented as,

$$\Delta G[* \text{CO}_2] = G[* \text{CO}_2] - (G[*] + G[\text{CO}_2])$$

$$\Delta G[* \text{COOH}] = G[* \text{COOH}] - (G[*] + G[\text{CO}_2] + G[\text{H}])$$

$$\Delta G[* \text{CO}] = G[* \text{CO}] + G[\text{H}_2\text{O}] - (G[*] + G[\text{CO}_2] + 2G[\text{H}])$$

$$\Delta G[\text{CO}] = G[\text{CO}] + G[\text{H}_2\text{O}] - (G[\text{CO}_2] + 2G[\text{H}])$$

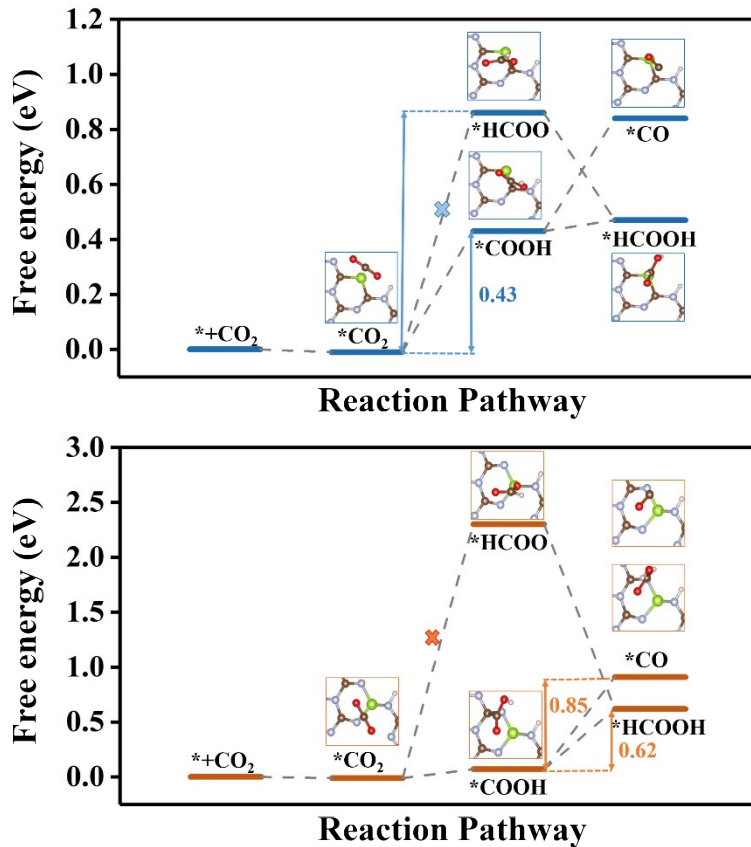


**Fig. S12.** Free energy diagrams for  $\text{CO}_2$  reducing to CO and  $\text{HCOOH}$  via a 2-ele process on (a)  $\text{SeN}_2$  (b)  $\text{SeC}_3$ .

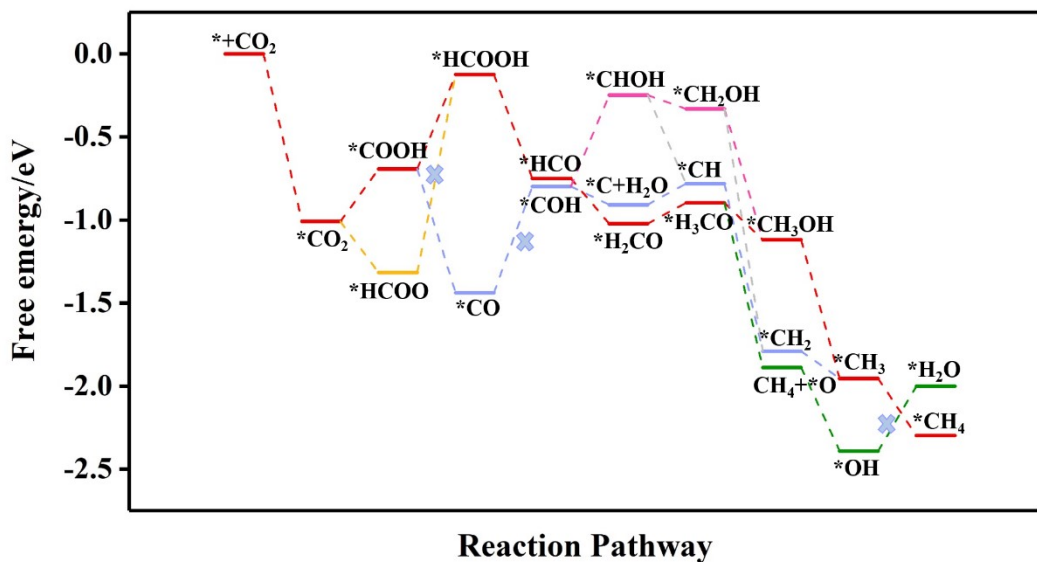


**Fig. S13.** Free-energy profile for  $\text{CH}_3\text{OH}$  and  $\text{CH}_4$  production of CRR on  $\text{Co}_4@\text{SeN}_2$ .

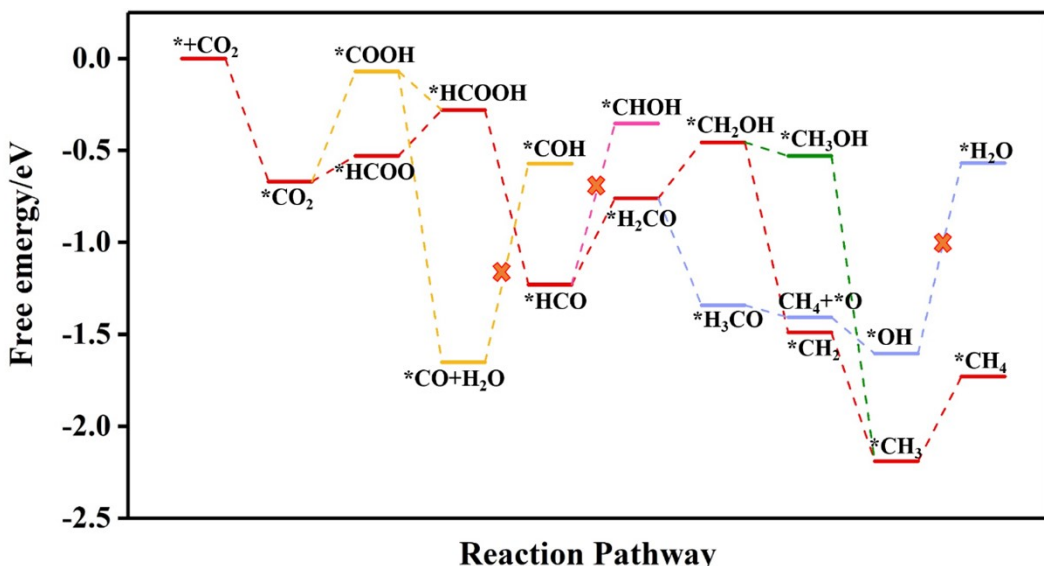


**Fig. S14.** Free-energy profile for  $\text{CH}_3\text{OH}$  and  $\text{CH}_4$  production of CRR on  $\text{Co}_4@\text{SeC}_3$ .